Available online at www.sciencedirect.com
ScienceDirect
Optics Communications 281 (2008) 846–850
OPTICS COMMUNICATIONS
www.elsevier.com/locate/optcom

Two-dimensional photonic crystals with pure germanium-on-insulator

M. El Kurdi [a], S. David [a], X. Checoury [a], G. Fishman [a], P. Boucaud [a,*], O. Kermarrec [b], D. Bensahel [b], B. Ghyselen [c]

[a] *Institut d'Electronique Fondamentale, CNRS Univ Paris Sud, Bâtiment 220, F-91405 Orsay Cedex, France*
[b] *STMicroelectronics, 850 rue Jean Monnet, 38920 Crolles, France*
[c] *Soitec, Parc technologique des fontaines, 38190 Bernin, France*

Received 19 July 2007; received in revised form 26 September 2007; accepted 3 October 2007

Abstract

We have investigated pure germanium two-dimensional photonic crystals. The photonic crystals which exhibit resonances in the near infrared spectral range were fabricated on germanium-on-insulator substrates using standard silicon-based processing. The germanium-on-insulator substrate consists of a thin layer of pure germanium-on-oxide deposited on a silicon substrate. The optical properties are probed by the direct band gap optical recombination of pure germanium at room temperature. Resonant optical modes are evidenced between 1.68 and 1.53 μm in different type of hexagonal cavities (H1–H5). The spectral position of the modes is controlled by the lattice periodicity and air filling factor of the photonic crystals. Close to the Ge band edge, the quality factors are limited by the bulk material absorption.

PACS: 42.70 Qs; 78.55. –m; 78.66.Db

Keywords: Photonic crystal; Germanium; Photoluminescence

1. Introduction

Very strong progress has been achieved over the past years in the field of silicon photonics either for passive or active devices. Cavities with record quality factors have been demonstrated by using photonic heterostructures fabricated in silicon membranes [1]. On-chip optical buffers with very long optical delays lines have been fabricated with microring resonators and group delays up to 500 ps with an ultracompact design have been reported [2]. Pulsed and continuous wave Raman lasers with silicon as the active medium have also been demonstrated [3]. These advances are not limited to pure silicon. A strong interest is also devoted to structures containing Ge since this material is compatible with the standard CMOS processing of the microelectronics industry. Ge/Si self-assembled islands can be used as internal sources to probe the optical properties of two-dimensional photonic crystals [4,5]. Pure Germanium is characterized by a very large refractive index (~4.1–4.2 in the near infrared as compared to 3.5 for silicon). It also exhibits a direct band gap around 0.8 eV at room temperature not far in energy from the indirect band gap (0.66 eV). This direct band gap results in strong absorption coefficients at 1.5 and 1.3 μm. Pure germanium photodetectors on silicon with very high cut-off frequencies and large responsivities have been demonstrated with this system [6,7]. Quantum confined Stark effects based on excitonic transitions with pure germanium quantum wells grown on relaxed buffer layers on silicon have also been

* Corresponding author. Tel.: +33 1 69 15 40 92; fax: +33 1 69 15 40 90.
E-mail address: philippe.boucaud@ief.u-psud.fr (P. Boucaud).

0030-4018/$ - see front matter © 2007 Elsevier B.V. All rights reserved.
doi:10.1016/j.optcom.2007.10.008

evidenced, opening the route to the development of electro-absorption optical modulators operating around 1.5 μm [8]. A lateral superlattice in germanium-on-insulator has been proposed for electrically pumped lasing at 1.55 μm [9]. Strained germanium has also been predicted to exhibit a direct band gap for tensile deformation greater than 2% [10].

In order to enhance the absorption, modulation, or emission properties of germanium-based structures, resonant cavities are particularly important. In this work, we have investigated two-dimensional photonic crystals fabricated on a germanium-on-insulator substrate. We show that cavities with resonances at wavelengths between 1.68 and 1.53 μm can be fabricated by using standard silicon processing. The photonic crystals were characterized by the room temperature photoluminescence of the bulk germanium which is associated with the direct band gap recombination. The spectral position of the resonant modes is controlled by the air filling factor of the photonic crystals and by the lattice periodicity of the triangular pattern.

2. Sample fabrication

The germanium-on-insulator substrate was obtained by wafer bonding using the Smart-Cut™ technology [11]. Hydrogen implantation is used to peel off a very thin layer of a germanium wafer which is later bonded on a silicon wafer covered by an oxide layer. Following this procedure, we obtain a 230 nm thick pure Ge layer separated by a 170 nm thick oxide from a silicon substrate. The bonding was done on a four inches wafer. The fabrication of the photonic crystals was performed with the same processing techniques used for the silicon-based photonic crystals. A 300 nm thick photoresist (ZEP520A) was first deposited on the sample. A triangular lattice pattern and hexagonal cavities were defined by electronic beam lithography. The pattern was then transferred into the germanium layer down to the buried oxide by reactive ion etching using SF_6 and CHF_3 gases. No oxygen was used in the process. The etch processing was optimized on bulk germanium layers grown on relaxed buffer on silicon, before being transferred to germanium-on-insulator substrates. Defect hexagonal cavities (H1–H5) were fabricated. This type of cavity is known to exhibit large losses and small quality factors. Moreover, the small thickness of the buried oxide and the asymmetry of the structure leads to a large leakage of the optical modes to the substrate and mixing between quasi-TE and quasi-TM modes. We have deliberately chosen to etch the structure only through the Ge layer, i.e. without etching the oxide nor the buried silicon substrate. It is indeed technologically more challenging to etch a stack of different layers (Ge, SiO_2, Si) while keeping a good homogeneity, verticality, and small roughness. Etching of the Ge layer is also appropriate for future membrane fabrication or the fabrication of photonic crystals on thick buried oxide.

3. Results

Fig. 1 shows a cross-section of the vertical stacking and a scanning electron micrograph image of a H1 cavity fabricated on a photonic crystal with a triangular lattice. The lattice periodicities and air filling factors of the photonic crystals were calculated in order to obtain a photonic band gap of the bulk two-dimensional structure covering the 1.8–1.5 μm spectral range. The bulk germanium index at these wavelengths is around 4.1–4.2 [12]. The large difference of index of refraction with the air or the oxide cladding leads to a better vertical confinement of the light as compared to the silicon-based photonic crystals. It also leads to the opening of a larger photonic band gap for the triangular lattice. For a 230 nm thick germanium layer on a 170 nm thick oxide, the effective index in TE polarization is 3.48 at 1.6 μm. Lattice periodicities between 460 and 540 nm with air filling factors between 42 and 55% were investigated. The optical properties were probed at room temperature with a microphotoluminescence set-up. The optical excitation was provided with a 458 nm line of an argon ion laser. The absorption coefficient of Ge at this wavelength is around 550,000 cm^{-1}[12], and all the light is absorbed in the first tens of nanometer of the upper germanium layer. The incident power on the sample is a few mW focused on a few μm diameter spot. The luminescence was excited and collected at normal incidence using an objective with a 0.6 numerical aperture. The microphotoluminescence spectra were analyzed with a nitrogen-cooled germanium detector. This detector has a very high sensitivity, its drawback is a cut-off at 0.77 eV (1.61 μm). This cut-off does not however prevent the observation of resonant emission peaks at long wavelengths.

At room temperature, the luminescence of both indirect band gaps and direct band gaps of germanium can be experimentally observed. The indirect band gap has a maximum around 0.67 eV (1.85 μm) while the direct band gap recombination has a maximum around 0.81 eV (1.53 μm). The energetic position of this maximum can depend on the reabsorption which remains quite small for a 230 nm thick layer. We emphasize that the ratio between radiative recombination associated with the direct band gap and the radiative recombination associated with the indirect band gap is around 4 at room temperature in bulk germanium [13]. It indicates that the amplitude of the direct band gap recombination is roughly four times larger around

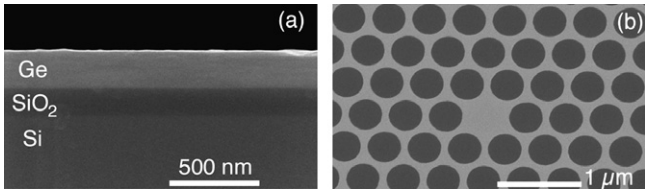

Fig. 1. (a) Scanning electron micrograph cross-section of the germanium-on-insulator substrate. (b) Scanning electron micrograph of a H1 cavity fabricated on the germanium-on-insulator substrate.

810 meV as compared to the indirect band gap recombination around 0.67 eV. Fig. 2 shows the room temperature photoluminescence spectra of H1 cavities for different lattice periodicities (460, 480 and 500 nm) and a nearly constant air filling factor (~55% corresponding to a radius over lattice periodicity $r/a = 0.39$ for the triangular lattice). These photoluminescence spectra are compared to the photoluminescence of the unprocessed germanium layer. In the latter case, the photoluminescence is resonant around 0.81 eV, and corresponds to the direct band gap recombination. The luminescence of the germanium-on-insulator layer obtained by wafer bonding is equivalent to the luminescence of a bulk germanium substrate. The photoluminescence of the H1 cavities is strikingly different from the luminescence of the unprocessed layer. A resonance is observed at long wavelength with a maximum which shifts towards low energy as the lattice periodicity is increased. The energetic position of the resonance corresponds to a normalized frequency $u = a/\lambda \sim 0.3$. The amplitude of the recombination varies linearly with the incident optical power density. A part of the germanium bulk emission is directly coupled to the radiative continuum as leaky modes and is thus equivalent to the emission of the bulk unprocessed layer. We have modeled the optical properties of the H1 cavity fabricated on the germanium-on-insulator substrate using a two-dimensional plane wave calculation and a three-dimensional finite difference time domain (3D–FDTD) calculation. The photonic band gap of the triangular lattice for the 500 nm lattice and $r/a = 0.39$ covers the 0.245–0.40 spectral range in normalized frequency, i.e. corresponding to 0.6–1 eV or 2.04–1.25 μm, respectively. Using an effective index of 3.48 for TE polarization at 1.6 μm in the 2D plane wave calculation, the dipolar mode of the H1 cavity is calculated at $u = 0.277$, a quadrupolar mode at $u = 0.35$, a monopole mode at $u = 0.373$ and a gallery mode at 0.394. The 3D–FDTD calculation predicts the dipolar mode at a larger energy ($u = 0.287$) than the 2D calculation, i.e. 0.712 eV instead of 0.765 eV measured experimentally for the 500 nm lattice. We note that the FDTD calculation accounts for the modal dispersion of the waveguide. The amplitude of the dipolar mode coupled to the continuum is significantly larger than the amplitudes of the other confined modes. We thus attribute the experimental resonance observed on the H1 cavities to the fundamental dipolar mode. The 7% discrepancy between the experimental and modeling resonance values is attributed to the uncertainty in the effective index value for the germanium-on-insulator substrate and a deviation from the nominal parameters. There is indeed a decrease of the refractive index at large photo-induced carrier densities which is not accounted for in the calculation. The absorption coefficient of bulk germanium varies significantly at the edge of the direct band gap. This absorption limits the value of the quality factor that can be achieved. Fig. 3 shows the dependence of the inverse of the quality factor as a function of the Ge absorption coefficient at the resonant wavelengths for the different H1 cavities. It exhibits, as expected, a linear dependence with a decrease of the quality factor as the material absorption increases [14]. The extrapolation of the inverse of the quality factor to zero absorption gives the intrinsic quality factor value ($Q \sim 85$) which corresponds to the one calculated by 3D–FDTD. We have modeled the properties of the cavities for different hole etch depths,

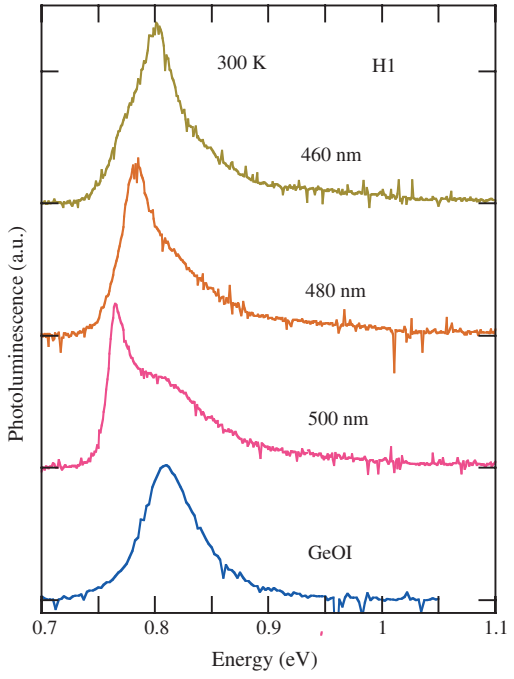

Fig. 2. Room temperature photoluminescence of the bulk germanium-on-insulator substrate and H1 cavities for different triangular lattice periodicities. The air filling factor is 55%. The curves have been offset for clarity. The lattice periodicities are indicated on the graph.

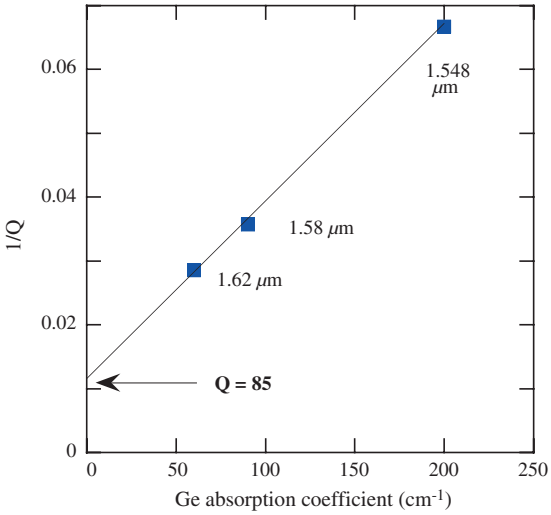

Fig. 3. Inverse of the quality factors of the resonant mode of different H1 cavities as a function of the bulk material absorption at the resonant wavelength. The quality factors and resonant wavelengths are extracted from Fig. 2. The full line is a linear fit. Its extrapolation to zero gives the intrinsic quality factor of the cavity, in agreement with the value calculated by 3D–FDTD.

as it is known that the etch thickness can have an impact on the out-of-plane losses of the photonic crystals [15]. Etching of the oxide layer does not change significantly the quality factors. The quality factor of the dipolar mode increases to 225 if the buried silicon, i.e. below the oxide layer, is further etched down to a 1.25 μm thickness. In the latter case, a better overlap between the vertical mode profile and the hole etch depth is obtained leading to a reduction of out-of-plane losses. A similar increase of quality factors can be obtained by fabricating the photonic crystals (i.e. only etching the Ge layer) on a thicker buried oxide layer. The quality factor of the dipolar mode increases up to 270 for an oxide thicker than 400 nm. As mentioned above, these standard H1 cavities are intrinsically lossy and it is beyond the scope of this letter to demonstrate very high quality factors on these novel germanium-on-insulator substrates. We note that for that purpose, the simple approach, technologically speaking, would be to study structures fabricated on a thick buried oxide or following the membrane approach. Meanwhile all strategies that have been recently proposed and demonstrated to realize nanocavities with very high quality factors like elongated cavities with shifted edge air holes or photonic heterostructures [16] could obviously be used for two-dimensional photonic crystals fabricated with germanium-on-insulator substrates. We note that the H1 cavities present a small modal volume V and despite their weak quality factor, the ratio Q/V which drives the Purcell enhanced recombination rate can be significant with this system.

Fig. 4 shows the photoluminescence spectra of a H2 hexagonal cavity measured for a fixed crystal periodicity and varying air filling factors. The lattice periodicity is 500 nm. Despite the cut-off of the germanium detector, optical modes can be observed at low energy corresponding to a significantly enhanced emission at long wavelength (1.65 μm ~ 0.75 eV). The quality factor of the optical modes decreases as the resonance emission gets closer to the germanium band gap because of the large absorption of the material. The resonant emission shifts as expected to long wavelength as the air filling factor decreases from 55 to 44%. The number of confined optical modes is much larger for the H2 cavity in a triangular lattice with large filling factors, and we do not attempt to identify the optical modes. The energy shift of the resonant emission from $u = 0.303$ to 0.314 is consistant with the shift that can be calculated for a given optical mode as a function of the air filling factor increasing from 44 to 55%. For a fixed air filling factor (55%) and varying lattice periodicities (460–540 nm), the position of the resonant peak is around 0.32 in normalized frequency and shifts to lower values as the lattice periodicity is decreased. This shift, similar to the one observed for the H1 cavity, is attributed to the change of index of refraction and to the variation of the modal index of the waveguide as the energy increases.

Fig. 5 shows the room temperature photoluminescence of hexagonal H5 cavities for different lattice periodicities and a constant air filling factor. At least three modes can be observed on the low-energy side of the spectrum for the cavity with a lattice periodicity of 520 and 500 nm. The normalized frequencies of these modes are around 0.295, 0.31 and 0.325. The number of confined optical modes in such a cavity is significantly larger than for H1 and H2 cavities, which explains in turn that more modes can be coupled to the radiative continuum above the light line. The quality factors of the optical modes are limited by the small thickness of the oxide layer which enhances the radiative loss to the substrate. The asymmetry of the structure which couples the TE and TM polarizations also contributes to in-plane radiation losses, a situation which is detrimental to the achievement of high quality factors [17].

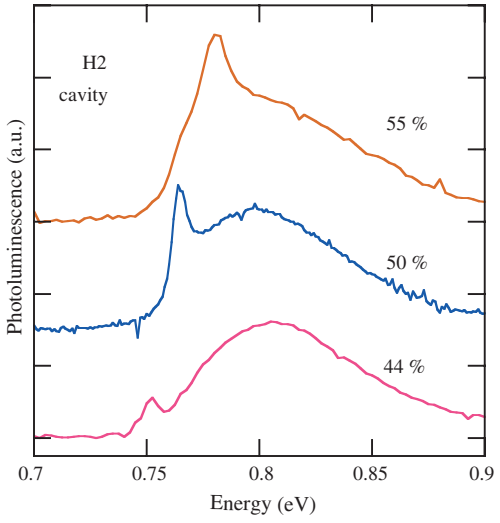

Fig. 4. Room temperature photoluminescence of a H2 cavity with a 500 nm lattice periodicity and different air filling factors (44, 50, 55%) indicated on the spectra.

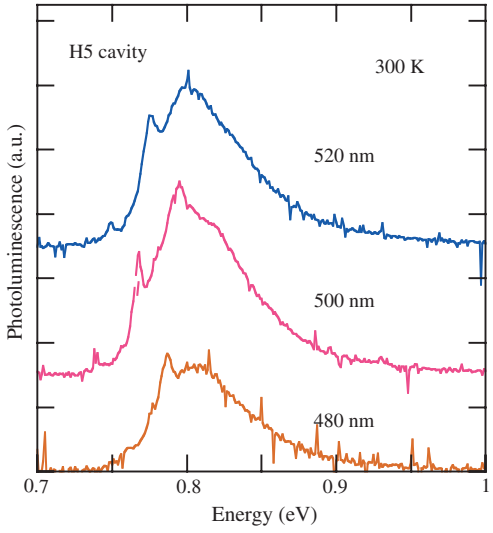

Fig. 5. Room temperature photoluminescence of H5 cavities with different lattice periodicities (480, 500, 520 nm). The air filling factor is 55%.

As shown above, the photonic crystals fabricated from germanium-on-insulator substrates can enhance the interaction at long wavelength, i.e. on the edge of the direct band gap absorption and emission. This could provide a path to circumvent the limitation to the use of germanium in integrated compact telecommunication or optoelectronic devices due to its weak absorption at 1.55 μm and above. As discussed in Ref. [10], tensily strained germanium might exhibit a direct band gap. This tensile strained material could be obtained for example by combining GeSn and GeSiSn heterostructures. The achievement of a direct band gap could lead to stimulated and laser emission with these heterostructures. Compact optical resonators to observe this stimulated emission could be obtained with two-dimensional photonic crystals like those demonstrated in the work. Germanium-on-insulator substrates would moreover represent an additional step to integrate these devices on a silicon platform. The fabrication and engineering of germanium-based photonic crystals appear therefore as a promising route for silicon and germanium photonics.

In conclusion, we have fabricated two-dimensional photonic crystals with pure germanium-on-insulator substrates. Germanium has a large index of refraction which is an advantage for engineering and designing photonic crystals. The optical emission associated with both indirect and direct band gaps at room temperature can also be used as an internal source to probe the optical properties of the photonic crystals. Different hexagonal cavities in a triangular lattice pattern have been investigated. Resonant optical modes have been observed around 1.6 μm on the low-energy side of the direct band gap absorption. The spectral position of the modes is controlled by the lattice periodicity and the air filling factor of the photonic crystals. The realization of pure germanium two-dimensional photonic crystals and the control of resonant optical modes is an important step in order to develop germanium photonics and cavity-enhanced devices with this material.

Acknowledgements

This work was supported by the French Ministry of Industry under Nano2008 convention. We thank T. Akatsu and C. Richtarch for the fabrication of the germanium-on-insulator substrates.

References

[1] B.S. Song, S. Noda, T. Asano, Y. Akahane, Nature Materials 4 (3) (2005) 207.
[2] F.N. Xia, L. Sekaric, Y. Vlasov, Nature Photonics 1 (1) (2007) 65.
[3] O. Boyraz, B. Jalali, Optics Express 12 (21) (2004) 5269.
[4] S. David, M. El kurdi, P. Boucaud, A. Chelnokov, V. Le Thanh, D. Bouchier, J.M. Lourtioz, Applied Physics Letters 83 (13) (2003) 2509.
[5] X. Li, P. Boucaud, X. Checoury, O. Kermarrec, Y. Campidelli, D. Bensahel, Journal of Applied Physics 99 (2) (2006) 023103.
[6] G. Dehlinger, S.J. Koester, J.D. Schaub, J.O. Chu, Q.C. Ouyang, A. Grill, IEEE Photonics Technology Letters 16 (11) (2004) 2547.
[7] M. Oehme, J. Werner, E. Kasper, M. Jutzi, M. Berroth, Applied Physics Letters 89 (7) (2006) 071117.
[8] Y.H. Kuo, Y.K. Lee, Y.S. Ge, S. Ren, J.E. Roth, T.I. Kamins, D.A.B. Miller, J.S. Harris, Nature 437 (7063) (2005) 1334.
[9] R. Soref, IEEE Journal of Selected Topics in Quantum Electronics 12 (6) (2006) 1678.
[10] R. Soref, J. Kouvetakis, J. Menendez, Material Research Society Symposium Proceedings 958 (2007) L01.
[11] T. Akatsu, C. Deguet, L. Snachez, F. Allibert, D. Rouchon, T. Signamarcheix, C. Richtarch, A. Boussagol, V. Loup, F. Mazen, J.M. Hartmann, Y. Campidelli, L. Clavelier, F. Letertre, N. Kernevez, C. Mazure, Materials Science in Semiconductor Processing 9 (4–5) (2006) 444.
[12] H.R. Philipp, E.A. Taft, Physical Review 113 (4) (1959) 1002.
[13] Y.P. Varshni, Physica Status Solidi 19 (1967) 459.
[14] I. Alvarado-Rodriguez, E. Yablonovitch, Journal of Applied Physics 92 (11) (2002) 6399.
[15] H. Benisty, D. Labilloy, C. Weisbuch, C.J.M. Smith, T.F. Krauss, D. Cassagne, A. Beraud, C. Jouanin, Applied Physics Letters 76 (5) (2000) 532.
[16] T. Asano, B.S. Song, Y. Akahane, S. Noda, IEEE Journal of Selected Topics in Quantum Electronics 12 (6) (2006) 1123.
[17] Y. Tanaka, T. Asano, R. Hatsuta, S. Noda, Applied Physics Letters 88 (1) (2006) 011112.